LASER SHOCK FRESH FUEL BOND STRENGTH STUDIES

J.A. Smith, C.L. Scott, B.H. Rabin
Measurement Science, Idaho National Laboratory
P.O. Box 1625, MS 2209, 83415, Idaho Falls, ID

1.   ABSTRACT

Laser-based characterisation of base monolithic U-10Mo fuel is being conducted by the USHPRR Fuel Qualification project to support fabrication development and ensure the fuel maintains mechanical integrity and does not delaminate during normal operating conditions. Characterisation involves laser shock experiments, combined with laser-ultrasonic scanning, to evaluate the bonding integrity and strength of interfaces within fuel plates. This report documents fresh fuel studies that were carried out on a series of fuel plates manufactured at Los Alamos National Laboratory in which various, controlled levels of interfacial contamination are intentionally introduced into the fuel plates during fabrication to vary the bond strength. Additional studies were conducted on developmental fuel plates supplied by the USHPRR Fuel Fabrication Pillar in which the Zr diffusion barrier was applied to the U-Mo foils by electroplating and plasma spraying. The electroplating and plasma spraying processes are being evaluated as alternatives to the baseline co-rolling fabrication process.

2.   Introduction

Under the United States High Performance Research Reactor (USHPRR) Fuel Qualification project at Idaho National Laboratory, laser-based characterisation techniques are being used to evaluate the bonding integrity and strength of interfaces in nuclear fuel plates, with a focus on the high uranium-density base monolithic U-10Mo fuel being developed to support conversion of research reactors from highly enriched uranium to low-enriched uranium fuel. Fresh fuel studies are being used to assess the impacts of fabrication variables on as-fabricated bond strength, and the ongoing hot cell implementation of these capabilities will enable post-irradiation bond strength measurements to be made, for comparison with as-fabricated bond strength. The primary goals of this work are to support fabrication process development and establish appropriate fuel product specifications, if necessary, to ensure that fuel plates maintain mechanical integrity and do not delaminate under normal operating conditions

3.   Overview of the Laser Shockwave Technique

The characterisation methods, equipment and techniques, advantages, limitations, etc., have been described in detail previously [1-7]. In general, the methods involve application of two complementary experimental techniques, laser-shockwave testing and laser-ultrasonic imaging, collectively referred to as the Laser Shockwave Technique (LST), which allows the integrity, physical properties and interfacial bond strength in fuel plates to be evaluated. Characterisation results include measurement of layer thicknesses, elastic properties of the constituents, and the location and nature of generated debonds.

In laser shock testing, a high-power pulsed laser is used to generate shock waves that interrogate the specimen. The shock wave travels as a compression wave through the material to the free (unconfined) back surface, and reflects back through the material as a rarefaction (tensile) wave. This tensile wave is the physical mechanism that produces internal failure (i.e. interfacial delamination) within the specimen. To enhance the efficacy of the optical-to-mechanical energy transfer [2-6], the surface of the specimen is covered with an optically

absorbing black tape and then covered with a transparent constraining medium as shown in Figure 1. The shock wave produced under the confinement cover produces high-amplitude molecular displacements on the surface of the aluminium cladding. To keep the plasma contained, a strong high-temperature transparent tape is used. The shock wave source size (roughly the laser spot size) needs to be about two times the sample thickness (about 1.5 mm) to approximate one-dimensional (1-D) wave propagation. Under the 1-D approximation, shear stresses are neglected, and the shock wave is exclusively compressive when first generated.
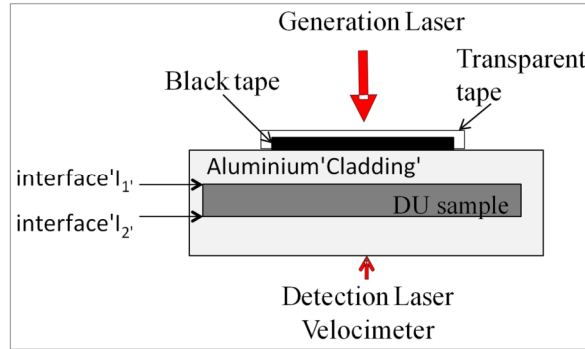

FIG. 1. The plate fuel specimen, geometries, plasma constraining mechanism and back surface velocity detection for laser shock testing is shown.

During testing of a fuel plate specimen, bond strength is determined by increasing the laser pulse energy incrementally, which increases the amplitude of the interrogating shockwave. The threshold stress value is imposed at the interface when debonding is imminent. The stress is indirectly calculated from the measured back-surface velocity, u, (see Figure 1) as recorded by an optical velocimeter based on a solid Fabry-Perot etalon [7]. Assuming 1-D, elastic wave propagation, and ignoring multiple reflections, the simplified relation between the back-surface velocity and interior stress is given by Eq. 1. [1-6].

$$\sigma(t) = \rho\, c\, u(t)/2 \qquad (1)$$

Where,

c = Speed of sound in Al (6.4 mm/µs; 6,400 m/s; measured)
ρ = Al 6061 density (2.70 g/cm³; 2,700 kg/m³)
$u(t)$ = Measured surface velocity (m/s)

Eq. 1 simply quantifies the maximum interior stress that makes it through the specimen to the back surface when the internal interfaces are intact. When an interface is debonded or has deteriorated, energy is dispersed or absorbed. While the shock wave energy reaching the back surface must have made it across at least partially intact internal interfaces, the actual stress field at the internal interface is more complicated, and may be higher or lower, due to specimen geometry effects and interaction of multiple reflections [1-3] from all interfaces.

To be able to identify debonding of the interfaces during a test, the LST system also contains a fully functional and independent laser-based ultrasonic (LUT) imaging subsystem. The LUT system is used to identify and image debonding caused during the laser shock test. The LUT system is capable of performing standard non-destructive evaluation and imaging functions such as microstructure characterisation, flaw detection and dimensional metrology in complex components via ultrasonic inspection techniques. LUT images made prior to and after the laser shock interrogation are used to confirm the presence of debonds, as well as to define the size and through-thickness location of debonds created. The LUT imaging is performed without tape or confinement and is similar to a conventional ultrasonic C-scan.

The LST system at Idaho National Laboratory (INL) has been developed for and is being used to study monolithic fuel plates consisting of U-10Mo alloy foil (typically 0.2 to 0.4 mm in thickness) having an approximately 25 µm Zr diffusion barrier coating and clad in aluminium alloy 6061 (AA6061) by a hot isostatic pressing (HIP) process [8], as shown schematically in

Figure 1. In the monolithic fuel system, the integrity and interfacial strength of the bond between the fuel and the aluminium cladding is important and is therefore the focus of this investigation. To determine the fuel-cladding interfacial strength, the shock laser energy will be increased until debonding is observed through LUT imaging, and the corresponding back-surface velocity is recorded. During a typical experiment, laser shockwave interrogation will be performed at several different locations on each fuel plate specimen. Details of the experimental procedure are presented below.

3.1   Materials

3.2   Variable Bond Strength Specimens

Los Alamos National Laboratory (LANL) fabricated and supplied to INL a series of fuel plate specimens in which fuel foils were fabricated by the baseline co-rolling process. The specimens included both fuel-cladding and cladding-cladding fuel plate segments. The intent of this fabrication work was to produce samples having variable bond strength, using either oxide or hydrocarbon contamination introduced in a controlled manner during the fabrication process. The resulting fuel plate bonds were evaluated by the bond strength measurement techniques under investigation by the program to access the capability for distinguishing bond strength variations due to potential process upset conditions. Upset conditions are anticipated in the production environment that may negatively influence as-fabricated bond strength. Details of the fabrication and characterisation of these specimens were documented by LANL in an internal LANL report.

Fuel-Cladding specimens supplied by LANL contained depleted uranium (DU) as the fuel. Testing was performed on the following specimens:

1. 4D5 – Thick oxide Al to Zr bond

2. 3C5 – Thick HC Al to Zr bond

3. 4A5 – Thin HC Al to Zr bond

4. 4E5 – As cleaned (thin native oxide layer)

3.3   Alternative Zr Coating Process Specimens

The USHPRR Fuel Fabrication (FF) Pillar supplied INL with several developmental fuel plate test specimens that were used for scoping studies. All the specimens consisted of DU fuel foils; however, the Zr diffusion barrier was applied using alternative fabrication processes under development by FF. Most specimens contained fuel foils that were Zr coated by an electroplating process at Pacific Northwest National Laboratory (PNNL), whereas one specimen contained two partial fuel foils that were Zr coated by plasma spray at LANL. All of these fuel plates were clad in 6061 Al by a HIP process conducted at the INL [8] with nominally identical conditions. The PNNL electroplated foils were clad in HIP run 102 while the LANL plasma spray foils were clad in HIP run 104. Details of the fuel foil fabrication process and Zr coating application for these fuel plate specimens are not known at this time. The following fuel plate test specimens underwent LST testing:

1. 102-C-2B (electroplated Zr, as-plated)

2. 102-D-2B (electroplated Zr, post-plating heat treatment)

3. 102-E-2B1 (electroplated Zr, as-plated, obvious Zr blisters on as-received foils)

4. 102-D-1 (electroplated Zr, as-plated)

5. 104-6 (plasma sprayed Zr, contained two partial foil pieces with unknown pedigree)

After the plates were processed by HIP at INL, they were given a light sanding treatment but were otherwise not surface machined to a specified final thickness. Interestingly, once the foils are processed by HIP into fuel plates, the plates made from the different types of Zr coated foils appear unremarkable and show similar characteristics when imaged by conventional UT.

3.4   Test Procedures

All testing was conducted in accordance with an approved INL internal test plan, which specifies the requirements (including quality assurance), detailed test procedures and data acceptance criteria for this work. For plate testing, the following containment layer and system verifications will be used. The standard sacrificial and constraining layers will be used and are black electrical tape and 3M #8547 transparent tape, respectively [2].

3.4.1   Fuel-Cladding Test Steps

An initial shot location is used to define the energy range (amp delay) to test subsequent points by increasing laser power at that location until debonding of the interface has been achieved. The test specimen is marked with test locations that have a minimum of 5 mm grid spacing to maximise the number of possible testing locations with respect to the fiduciary mark F1 (lower left corner). See Figure 2 and Table 1. Each location is tested until interface failure by gradually increasing laser energy from the minimum value defined at the initial shot location in steps of -5 μs for the flash lamp delay. Standard LST testing is performed on the matrix locations in Table 2 with the specimen in standard orientation as defined below.
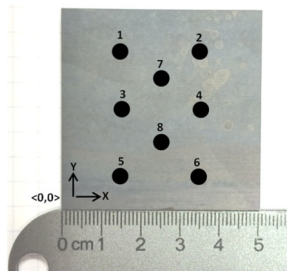

FIG 2. Example of fuel-cladding test fuel plate with locations for shock test indicated.

Fuel-cladding Test Fuel Plate **Shot Points**								
#	1	2	3	4	5	6	7	8
Location x, y (mm)	15, 40	35, 40	15, 25	35, 25	15, 10	35, 10	25, 32	25, 17

Tab 1: Example of fuel-cladding test fuel plate shock location.

3.5   Specimen Geometry and Nomenclature

To simplify the discussions that follow, the naming conventions for referring to sample orientation and interfaces used in stress calculations are shown schematically below in Figure 3. It's important to note that the identifying aspects of the fuel plate (e.g. front surface, interface I2, back cladding etc.) are established relative to the plate identification (ID) and is independent of the orientation of the fuel plate as measurements are being made.
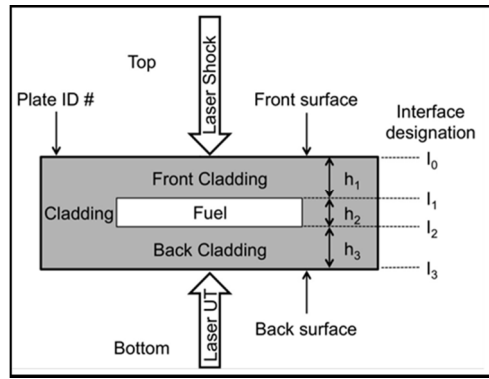
Fig 3. Diagram showing the plate geometry and nomenclature used for laser shock testing.

Alternatively, in the experimental reference frame, the laser shock is always carried out at the top of the specimen and velocimeter and LUT measurements are always performed from the bottom of the specimen. The reference or standard orientation is considered to be the case where the plate ID is facing up, i.e. it faces the shock laser, and the flipped orientation is where the plate ID is facing down, facing the velocimeter and laser-UT detection system.

4.   Results and Discussion

4.1   Fuel-Cladding Interface in Variable Bond Strength Specimens

Thus far, all LST testing of fuel plate specimens containing dissimilar interfaces have produced debonds. This was also the case with LANL-fabricated specimens tested in this work. The plates came in unfinished and the plates were machined down to thicknesses of 1.65 mm prior to LST testing. The resulting ultrasonic C-scans showed the same distinct signals and signatures as observed historically [2-6].

Figure 4 shows the resulting maximum surface velocities obtained for the LANL variable contamination specimens. The reference specimen is 4E5 with the Zr coating that was cleaned using typical procedures prior to HIP. The contaminated samples 4D5 and 4A5 show some interface strength degradation, which might be expected. Sample 3C5 with a thick hydrocarbon layer shows a slight increase in interface strength with respect to reference specimen 4E5.
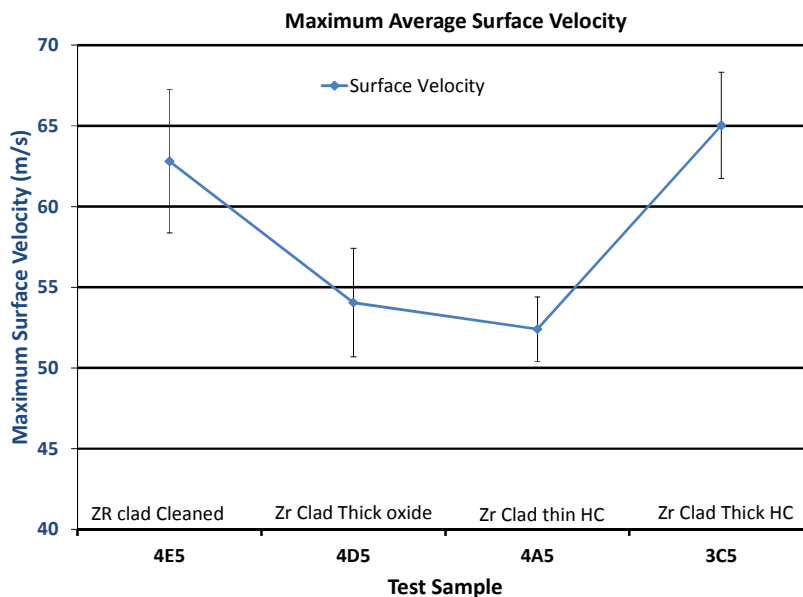

Fig 4. This graph shows the measured maximum surface velocity measured in the various LANL interface samples with varying levels of contamination.

The debond areas for the variable strength specimens are shown in Figure 5. In most laser shock samples tested to date, the maximum debond area is on the order of the incident shock laser beam diameter, and may be smaller depending on the severity of the debonding force. As shown in Figure 5, the debond area in these specimens was typically less than the incident shock laser beam size that had a diameter of 2-3 mm.
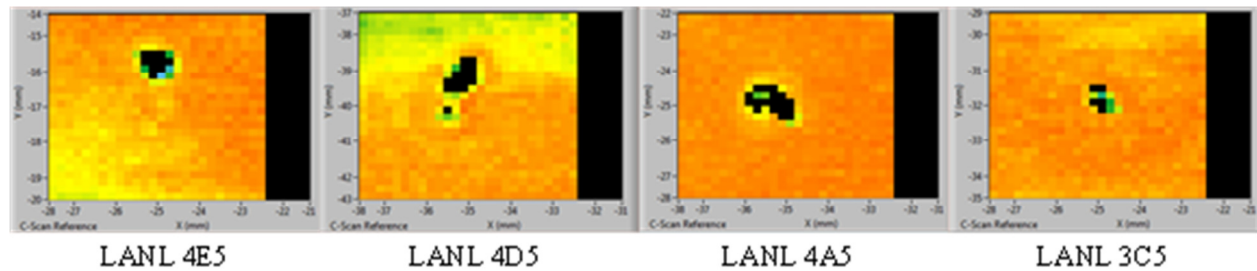

LANL 4E5   LANL 4D5   LANL 4A5   LANL 3C5

Fig 5. Representative images of the colourized debond locations in LANL plates caused by laser shock testing are shown. Note: The images are not to scale and debond size has to be determined from the scale in each image.

Using the simplified formula given in Equation 1, the debond threshold velocities can be converted to internal stresses and an estimate of the threshold for the interface strength can be determined as shown in Table 3. The internal stress given in the table is the highest stress obtained before the interface debonded. For comparison, the general mechanical properties for AA6061-O are the following [9]: Ultimate Tensile Strength, 160 MPa and Yield Strength, 79 MPa. Keep in mind that properties determined at high strain rate are different than properties measured during conventional low strain rate testing, therefore a direct comparison with reported tensile properties is not appropriate. In general, the materials can handle significantly higher dynamic stresses due to loss mechanisms such as dissipation (viscous loss) and conversion to heat. While correlations between the stresses measured at high strain rate and those determined by LST are still being investigated, the interface strengths determined by LST provide useful relative comparisons.

Specimen	Maximum Velocity (m/s)	Standard Deviation (m/s)	Internal Stress (MPa)	Deviation (MPa)
4E5	62.8	4.4	543	38
4D5	54.0	3.4	467	29
4A5	52.4	2.0	453	17
3C5	65.0	3.3	562	29

Tab 2: Maximum velocities are converted into estimates for the threshold interface debond strength at high strain rate for the variable bond strength fuel plate specimens produced by LANL.

4.2   Fuel-Cladding Interface in Alternative Zr Coating Processes Specimens

The plates with the electroplated and plasma Zr coatings are shown to have interface strengths that are in the range of 25% to 50% of the co-rolled foils. Figure 6 shows that the maximum back-surface velocity for the plated and plasma coatings ranges from 15 to 30 m/s, while the co-rolled plates have a range from 53 to 65 m/s as shown in Figure 4. The lowest maximum velocities near 20 m/s are near the lower limit of where the LST system is able to make reliable measurements. The debond areas for most of the alternative Zr coated plates are generally typical and are less than the 2-3 mm incident shock laser beam diameter, as shown in Figure 7. The atypical specimen is plate 102-E-2B1 that contains the foil that had obvious Zr coating blisters and discolouration in the as-received condition. The debond area for 102-E-2B1 has a diameter close to 8 mm, which is significantly larger than the incident shock laser spot size. As expected, plate 102-E-2B1 also exhibited the weakest fuel-cladding interface. The plasma sprayed foil in plate 104-6 also exhibited a weak interface, showing a bond strength comparable to that observed for blistered Zr coated electroplated foil in plate 102-E2B1.
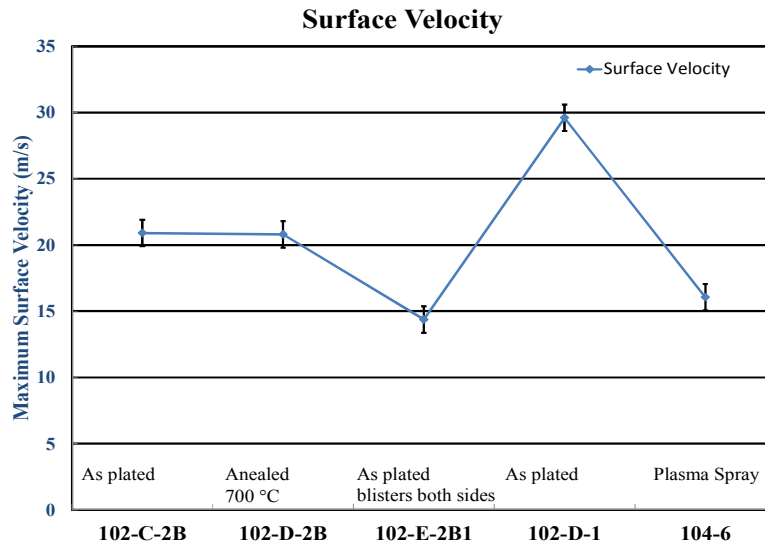
Fig 6. This graph shows the measured maximum surface velocity measured in the various PNNL interface samples with variable process parameters. The fuel plates contain the corresponding fuel foils: 21C-2B, 21D-2B, 21E-2B1, 21D-1.
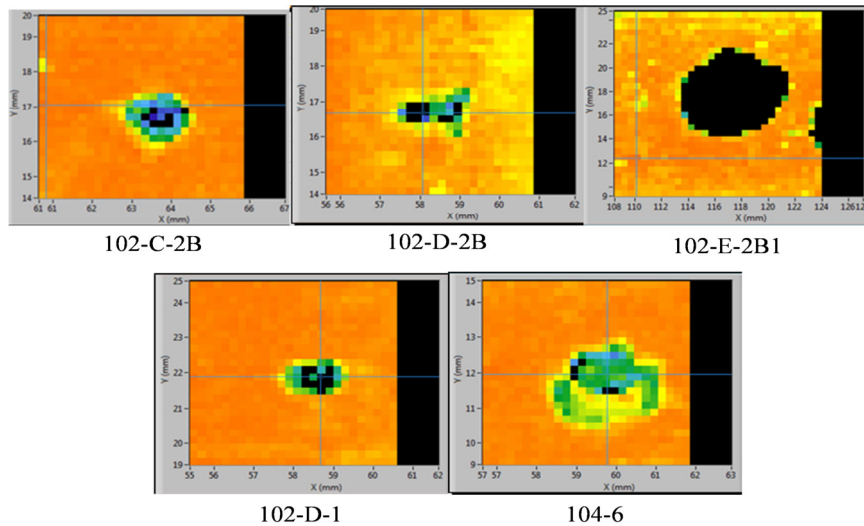

Fig 7. Representative images of the colourized debond locations caused by laser shock testing in PNNL plates are shown. Note: The images are not to scale and debond size has to be determined from the scale in each image.

The strongest fuel-cladding bond was observed for foil 21D-1. It is unknown what changes were made in the electroplating process for this foil, if any, were made. Assuming that as-plated foil 21C-2B can be considered the reference condition for electroplated Zr, it would appear that annealing the foil (annealing process details not available) after electroplating but prior to HIP had no significant influence on the interface strength, as shown by annealed foil 21D-2B in Figure 6. The conversion of maximum velocities to stress via Equation 1 is shown in Table 4. The debond stress for the electroplated foils are significantly lower than the co-rolled foils listed in Table 3.

The debond images of the four electroplated plates and the plasma-spray plate after LST testing are shown in Figure 7. These LST plates are much more interesting to review. The dark regions indicate debonds in interfaces that reflect sound and keeps sound from traveling through the fuel plate to the other side. With the exception of plate 102-E-2B1, these debond images are typical of debonds caused by LST, being on the same order as the incident shock laser spot size. While the HIP process appears to have healed the coating blisters on foil 21E-

2B1, the bond strength is low and the debond areas are large. Note that the exceptionally large debond areas for foil 21E-2B1 correspond to the blistered side of the foil (confirmed by reviewing the HIP can loading pictures); however, the interface strength appears to be similar on both halves (left and right) of the plate.

It is also interesting to note that the plasma spray foil has a slightly higher bond strength value than the blistered foil and has a typical debond area less than 2 mm. This is an indication that there is an additional failure mechanism in the plate made with the blistered foil 21E-2B1, such that the debond size is influenced by more than just the measured bond strength. At present, it is unknown what the additional mechanism might be, however, continued crack propagation along a particularly weak or brittle interface after passage of the tensile shock wave that results in initial debonding could explain these results.

PNNL Specimen	Maximum Velocity (m/s)	Standard Deviation (m/s)	Internal Stress (MPa)	Deviation (MPa)
102-C-2B	20.9	7.0	181	60
102-D-2B	20.8	4.9	180	42
102-E-2B1	14.4	2.8	124	24
102-D-1	29.6	2.6	256	22
104-6 LANL plasma	16.1	4.0	139	35

Tab 3: Maximum velocities are converted into estimates of threshold interface high strain rate debond strength for the plates supplied by the FF Pillar.
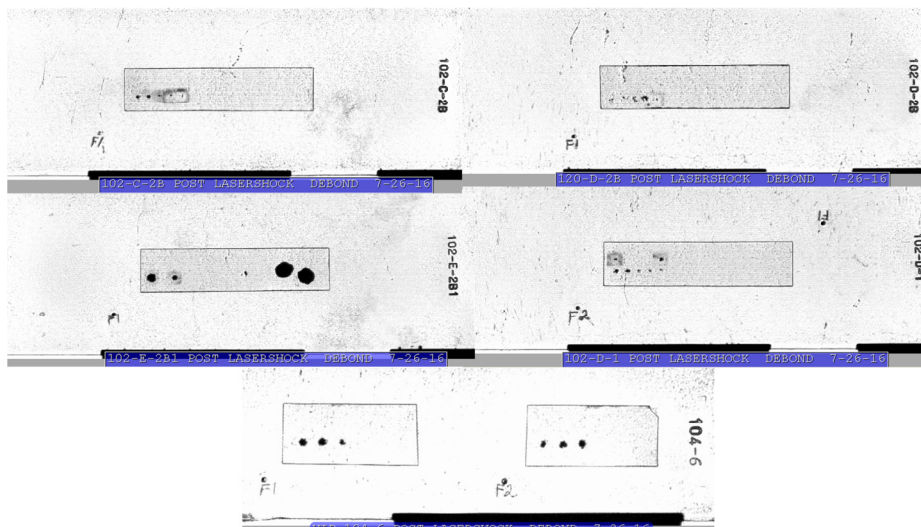

Fig 11. Ultrasonic C-scan images of the fuel plates provided by the FF Pillar that have been laser shock tested. The dark regions indicate debonds in interfaces that reflect sound and keeps sound from traveling through the fuel plate to the back side. While the HIP process appears to have healed the coating blisters on foil 21E-2B1, the bond strength is low and the debond areas are large. Note that the exceptionally large debond areas for foil 21E-2B1 corresponds to the blistered side of the foil.

5. Summary

One of the goals of the USHPRR project is to develop a fuel plate manufacturing process that delivers fuel plates having robust and reliable fuel-cladding interfacial strength. The goal of the LST testing technique is to develop a reliable and easy-to-perform method to quantify the fuel-cladding interface strength, allowing relative comparisons to be made between fabrication variants, as well as pre- and post-irradiation. One critical step in the manufacturing process is the application of the Zr coating. As discussed in this report, bond strength testing has been performed on fuel plates manufactured at LANL using the baseline co-rolling Zr application process foils, on fuel plates with Zr electroplated foils processed at PNNL and Zr plasma

sprayed foils processed at LANL. Another significant concern relates to the cleanliness of the plate surfaces during the manufacturing of fuel plates, which was also evaluated in this study.

In addition to a nominally cleaned reference co-rolled Zr fuel plate specimen, several plates were tested having various surrogate contaminants (hydrocarbon and oxide) and different levels of contamination. The results from LST testing are somewhat surprising, suggesting that contamination introduced during manufacturing did not negatively impact the fuel-cladding bond strength. These results are corroborated by interfacial fracture energy measurements made on specimens from the same fuel plates by bulge testing at LANL. The experimental uncertainty in the data is too large to quantify differences between the different samples but it is clear that the type of surface preparation or lack thereof had little effect on the resulting interface strength.

The present results also suggest that Zr co-rolled foils have significantly stronger fuel-cladding interfaces compared to either Zr electroplated and Zr plasma sprayed foils by 200% to 300%. Another surprising result is that the fuel plate containing a Zr electroplated foil that had obvious Zr blisters in the as-received (prior to HIP) condition exhibited a debond area at least twice the size of the incident shock laser spot size used to generate the debond, whereas typically, the debond area is less than the incident shock laser spot size. The Zr plasma spray specimen has a slightly higher bond strength value than the blistered Zr electroplated specimen and yet has a debond area less than the incident shock laser spot size, as is typical in LST testing. This is an indication that there is an additional failure mechanism in the plate made with the blistered Zr foil. Microscopy was performed on one LST location in the 102-D-1 electroplated plate. The interface separated at the Zr layer from the DU fuel foil. This is an indication that the Zr and Al interface is the weakest

6.   Acknowledgements

7.   References

1.   Smith, J.A., Rabin, B.H., Perton, M., Lévesque, D., Monchalin, J.-P., Lord, M., "Laser Shockwave Technique for Characterization of Nuclear Fuel Plate Interfaces," RERTR 2012— 34th International Meeting on Reduced Enrichment for Research and Test Reactors, Warsaw Marriott Hotel Warsaw, Poland, October 14-17, 2012.

2.   Smith, J.A., Rabin, B.H., Perton, M., Lévesque, D., Monchalin, J.-P., Lord, M., "Laser Shockwave Technique for Characterization of Nuclear Fuel Plate Interfaces," Review of Progress in Quantitative Nondestructive Evaluation, Vol. 1511, Denver CO, July 15-20, 2012, Thompson, D.O., Chimenti, D. E., Editors, American Institute of Physics, Melville, NY, PP. 345-352, 2013.

3.   Smith, J.A., Cottle, D.L., Rabin, B.H., "Laser Shockwave for Characterizing Diffusion Bonded Interfaces," Review of Progress in Quantitative Nondestructive Evaluation, Vol. 1581, Baltimore MD, July 21-26, 2013, Chimenti, D. E., Editor, American Institute of Physics, Melville, NY, PP. 999-1006, 2014.

4.   Smith, J.A., Cottle, D.L., Rabin, B.H., "Laser-Based Characterization of Nuclear Fuel Plates," INL's 2013 Nuclear Fuels & Materials Spotlight, Vol. 4, PP. 31-40, April 2014. Invited, INLNFMSpotlight@INL.gov.

5.   Lacy, J.M., Smith, J.A., Cottle, D.L., Rabin, B.H., "Developing a Laser Shockwave Model for Characterizing Diffusion Bonded Interfaces," Review of Progress in Quantitative Nondestructive Evaluation: Vol. 1650, Boise ID, July 20-25, 2014, D. E. Chimenti, Editors, American Institute of Physics, Melville, NY, PP. 1376-1385, 2015.

6.   Smith, J.A., Lacy, J.M., Lévesque, D., Monchalin, J.-P., "Use of the Hugoniot Elastic Limit in Laser Shockwave Experiments to Relate Velocity Measurements," Review Of Progress In Quantitative Nondestructive Evaluation, Vol. 1706, Minneapolis, MN, July 25-31, 2015, D. E. Chimenti, Editors, American Institute of Physics, Melville, NY, AN: 080005, 2016.

7.   Perton M., Blouin, A., Monchalin, J.-P., J. Phys. D: Appl. Phys., 44, 2011.

8.   Jan-Fong Jue, Blair H. Park, Curtis R. Clark, Glenn A. Moore, Dennis D. Keiser, Jr., "Fabrication of Monolithic RERTR Fuels by Hot Isostatic Pressing", Nuclear Technology, Volume 172, Number 2, Pages 204-210, November 2010.

9.   Makeitfrom.com. (Copyright 2009). 6061-O Aluminum, http://www.makeitfrom.com/material-properties/6061-O-Aluminum.